J S Afr Vet Assoc . 2022;93(1)
https://doi.org/10.36303/JSAVA.2022.93.1.500

J S Afr Vet Assoc
ISSN 2224-9435 EISSN 1019-9128

ORIGINAL RESEARCH

Heavily T2-weighted imaging findings of spinal cord swelling in dogs with intervertebral disc extrusion

N Sekiguchi, D Ito, C Ishikawa, N Tanaka, M Kitagawa

Laboratory of Veterinary Neurology, School of Veterinary Medicine, Nihon University, Japan
Corresponding author, email: *itou.daisuke@nihon-u.ac.jp*

This study investigated causes of attenuation of cerebrospinal fluid (CSF) signal on heavily T2-weighted (T2W) images in dogs with thoracolumbar disc extrusion. Medical records and magnetic resonance images were retrospectively reviewed. Dogs were classified into the following grades; grade 1, non-ambulatory paraparesis; grade 2, paraplegia with deep pain perception and grade 3, paraplegia without deep pain perception. The length of intramedullary T2W hyperintensity of the spinal cord, cranial/caudal expansion of extradural compressive materials (ECM), and the CSF signal attenuation were measured. Ratios to the second lumbar vertebra (L2) were calculated for the length of intramedullary T2W hyperintensity (T2W:L2), cranial/caudal expansion of ECM (ECML:L2), and CSF signal attenuation (CSF:L2). The dogs were classified into focal or extended T2W hyperintensity groups according to the length [focal, shorter than length of L2; extended, longer than L2]. The area of EMC and the spinal canal were measured on transverse images at the lesion deriving occupancy ratio. The correlation between CSF:L2 and other data were analysed, and CSF:L2 was compared between the grades. In dogs with intramedullary T2W hyperintensity, the locations of CSF attenuation and the hyperintensity were compared if those locations were matched. Fifty-five dogs were included, 36 of which showed intramedullary T2W hyperintensity. Twenty-two of 36 dogs were considered as match of the location of the CSF attenuation and hyperintensity. CSF:L2 was significantly correlated with T2W:L2 in dogs with extended T2W hyperintensity ($p = 0.0002$), while CSF:L2 was significantly correlated with ECML:L2 in dogs with focal or no T2W hyperintensity ($p = 0.0103$ and $p = 0.0364$, respectively). CSF:L2 in grade 3 was significantly greater than those in patients who were grade 1 or 2 (both $p < 0.001$). In conclusion, higher CSF:L2, which was frequently seen in grade 3, would be most consistent with a higher T2W:L2 which might indicate spinal cord swelling.

Keywords: canine, CSF, heavily T2W, FASE, MRI, myelography

Introduction

Thoracolumbar intervertebral disc extrusion (TL-IVDE) is a common spinal disease in dogs. Magnetic resonance imaging (MRI) and myelography findings have been published previously to predict prognosis in TL-IVDE dogs without deep pain perception (DPP) (De Risio et al. 2009; Duval et al. 1996; Ito et al. 2005; Levine et al. 2009). Extended spinal cord swelling due to intramedullary haemorrhage, oedema, inflammation, and necrosis, which can be recognised as a hyperintensity of the spinal cord parenchyma on T2-weighted (T2W) MRI images (Ito et al. 2005; Levine et al. 2009) or as attenuation of the subarachnoid contrast medium in myelography (Duval et al. 1996), is found to be associated with poor clinical outcome. Dogs with intramedullary T2W hyperintensity on mid-sagittal MRI or attenuation of the subarachnoid contrast medium on myelography more than three or five times the length of the second lumbar vertebral body (L2), respectively, were associated with a poor prognosis. Conversely, dogs with focal intramedullary T2W hyperintensity (less than the length of L2) or a lack of intramedullary T2W hyperintensity on MRI had better outcomes after surgical decompression. In addition, the presence and length of the intramedullary T2W hyperintensity has been reported to be associated with neurological severity in dogs with TL-IVDE (Boekhoff et al. 2012; Ito et al. 2005).

Imaging using single-slice heavily T2W MRI can provide anatomic information about the subarachnoid space without contrast medium (Nagayama et al. 2002). With heavily T2W sequences, the echo time (TE) is drastically lengthened so that the transverse magnetisation from short T2 molecules (nearly all tissues in the body except water, such as cerebrospinal fluid [CSF]) is almost completely lost, resulting in an absence of signal. Since water has a long T2 relaxation time, it can retain most of its transverse magnetisation and continue to appear hyperintense (Duncan & Amrhein 2012). Therefore, on so-called "MR myelography" images, CSF in the subarachnoid space is hyperintense and 'white', while the signals of the background (from fat, bone, or paravertebral soft tissue) are suppressed. In human studies, single-slice MR myelography was performed using a single thick slice (about 50 mm) (Aggarwal et al. 2012; Nagayama et al. 2002), and required no postprocessing to provide a projection image with excellent suppression of background signals. In addition, single-slice MR myelography images are acquired in a short time, as low as 30 seconds, therefore this sequence can be readily added to routine MRI examinations of the spine in humans (Aggarwal et al. 2012; Nagayama et al. 2002). In dogs with spinal cord diseases including IVDE, progressive myelomalacia (PM), spinal neoplasia, arachnoid diverticula, and meningomyelitis (Gilmour et al. 2017; Guillem Gallach et al. 2011; Ito et al. 2020; Mankin et al. 2012; Pease et al. 2006; Seilar et al. 2012), utilisation of this sequence has been reported. In dogs with IVDE, heavily T2W sagittal images could be used to localise the clinically significant lesion site by identifying attenuation the CSF signal caused by extradural compression due to extruded disc material.

(Guillem Gallach et al. 2011; Mankin et al. 2012). Two other studies have shown that dogs with TL-IVDE and concurrent PM have more extensive attenuation of the CSF signal on heavily T2W images (Castel et al. 2017; Gilmour et al. 2017) in comparison to dogs without PM. However, no previous study has evaluated if the CSF signal attenuation on heavily T2W images is associated with neurological severity or clinical outcomes after surgical decompression in dogs with TL-IVDE, nor the underlying mechanism of attenuation (compression by extradural material only, or by spinal cord swelling).

We hypothesised that the length of CSF signal attenuation on heavily T2W images would be longer in dogs without DPP that have extended hyperintensity of the spinal cord parenchyma on T2W images, as would be seen in cases of PM (Gilmour et al. 2017). The finding of T2W hyperintensity might indicate spinal cord swelling after spinal cord contusion due to disc material extrusion, and the presence of extended spinal cord swelling could narrow the subarachnoid space and lead to attenuation of the CSF signal on heavily T2W images. Conversely, dogs without extended intramedullary T2W hyperintensity of the spinal cord (focal or lack of intramedullary T2W hyperintensity), the attenuation in CSF signal on heavily T2W images would be focal and caused by extradural cord compression by extruded disc material. It has been reported that elevated protein concentrations and increased cell populations in CSF have resulted in attenuation of the CSF signal on heavily T2W images in dogs with meningomyelitis (Pease et al. 2006). Therefore, the changes in CSF composition in dogs with TL-IVDD, especially dogs with extended intramedullary T2W hyperintensities, could affect the attenuation of CSF signals on heavily T2W images, resulting in a mismatch between the location of the intramedullary T2W hyperintensity and the attenuation of the CSF signal.

We investigated whether the length of CSF signal attenuation on heavily T2W images would be correlated with i) the length of intramedullary T2W hyperintensity of the spinal cord; ii) extent of distribution of extradural compressive material (ECM) within the vertebral canal; and iii) neurological severity. In dogs with intramedullary T2W hyperintensity, iv) we evaluated whether the location of the T2W hyperintensity and attenuation of the CSF signal were the same in each case. In addition, we evaluated if v) extended attenuation of the CSF signal on heavily T2W images would be associated with poor clinical outcome following decompressive surgery.

Materials and methods

Case selection

The medical records of our hospital between January 2011 and December 2019 were retrospectively reviewed for dogs with non-ambulatory paraparesis or paraplegic dogs diagnosed with TL-IVDE. The patients were included in this study if the following data were available: neurological examination results, presurgical MR images, histopathological diagnosis of disc material, and follow-up information for at least six months. The diagnosis of TL-IVDE was made based on MRI examination and histopathological findings. Dogs with concurrent PM were included in this study regardless of whether they underwent surgery or not because of the associated poor prognosis. The presence of PM was presumptively diagnosed with MRI findings when intramedullary T2W hyperintensity of the spinal cord more than six times the length of the L2 vertebral body (Okada et al. 2010) was present, progressive ascending and descending neurological deficits (e.g. loss/decrease of myotatic, perineal, and panniculus reflexes, progressive loss of postural reaction in the thoracic limbs, and respiratory failure), or if the diagnosis was confirmed histopathologically by inspection of the spinal cord at *post-mortem* examination. Dogs with multiple lesions and/or hydrated nucleus pulposus extrusion were excluded.

Signalment and neurological severity

Breed, sex, age, body weight, results of neurological examination, lesion site, times between onset of clinical signs and MRI examination, MRI examination and surgery, and onset of clinical signs and surgery were all recorded. All dogs were classified into one of the following three groups depending on their presurgical neurological severity: grade 1, non-ambulatory paraparesis; grade 2, paraplegia with DPP; and grade 3, paraplegia without DPP. Loss of DPP was defined as the lack of any detectable behavioural response (e.g. crying, turning of the head, or biting) when the bones of all the digits of the hindlimbs or the tail were compressed with a pair of forceps. CSF analysis, if available, was reported and included the colour, cell population, specific gravity, pH, concentration of protein and glucose, and if blood contamination was present, to investigate if the changes in CSF composition would affect the attenuation of CSF signal on heavily T2W images.

MRI evaluation

All MRI sequences including heavily T2W were acquired using a 1.5-Tesla scanner (EXCELART Vantage, Canon Medical Systems Corp., Tochigi, Japan) and a spinal coil (CTL-array coil, Canon Medical Systems Corp., Tochigi, Japan). The dogs were positioned in dorsal recumbency. Sagittal and transverse T2W and T1W images were obtained with the following parameters: sagittal images (repetition time [TR], 3500 [T2W] or 450 [T1W] msec; TE, 120 [T2W] or 15 [T1W] msec; field of view [FOV], 30–35 cm × 25 cm; matrix, 224 × 384; slice thickness, 2 mm), transverse images (TR, 4000–5000 [T2W] or 590–735 [T1W] msec; TE, 120 [T2W] or 15 [T1W] msec; FOV, 18 cm × 18 cm; matrix, 256 × 256; slice thickness, 3 mm). Sequential continuous transverse T2W and T1W images were obtained of the entire lesion site. Heavily T2W images (dorsal single-slice MR myelography) using two-dimensional fast advanced spin echo (FASE) sequences (see Appendix for brand names of equivalent sequences in other MRI manufacturers), which is a brand name of sequence by Canon Medical Systems Corp., is used routinely at our institution in patients undergoing spinal MRI to facilitate appropriate positioning and to plan the subsequent sequences (TR, 6000 msec; TE, 1000 msec; slice thickness, 50 mm; FOV, 30 cm × 30 cm; matrix, 512 × 512; imaging time, approximately 50 sec).

All images were reviewed independently by two board-certified neurologists (M.K. and D.I.) and a radiologist (C.I.), who were blinded to the information of patients apart from the lesion site, using a commercially available DICOM viewer (OsiriX

ver.24, Newton Graphics, Inc., Hokkaido, Japan). The reviewers measured the following values: length of the L2 vertebral body (on sagittal T2W), longitudinal ECM (sagittal T2W), attenuation of CSF signal (dorsal FASE) and intramedullary T2W hyperintensity of the spinal cord (sagittal T2W), and areas of ECM and the spinal canal (transverse T2W). Each dog was measured once by each reviewer, and the mean values of the measurements taken by three reviewers were used for statistical purposes.

On sagittal T2W images, the length of L2 and length of the ECM were measured. If the reviewers visualised intramedullary T2W hyperintensity of the spinal cord (when compared to the remainder of the spinal cord), the length was measured (total length as well as cranial and caudal distance from the lesion centre where the spinal cord was most compressed by ECM). If the reviewers were not confident of the existence of an intramedullary T2W hyperintensity after evaluating the sagittal images, then the transverse T2W images were also reviewed. In all transverse images in which the intramedullary T2W hyperintensity was confirmed, the slice located at the cranial end and the slice located at the caudal end were selected. The sites of the two slices were linked on mid-sagittal T2W images and the distance between them was measured.

All dogs that showed intramedullary T2W hyperintensity were classified into one of the following two groups according to the length of the intramedullary T2W hyperintensity (Boekhoff et al. 2012; Ito et al. 2005; Levine et al. 2009): 'extended' intramedullary T2W hyperintensity group – the length of intramedullary T2W hyperintensity is more than the length of the L2; or 'focal' intramedullary T2W hyperintensity group – the length is less than the length of the L2.

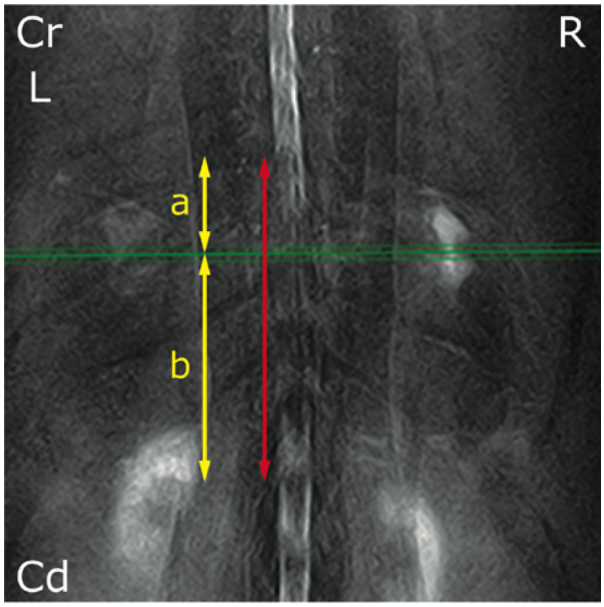

Figure 1: A dorsal FASE image from a dog with intervertebral disc extrusion. The green bar is the locator indicating the lesion centre where the spinal cord was most compressed by extradural compressive material. The length of the continuous cerebrospinal fluid signal attenuation at the lesion site is measured (red arrow), of which the cranial (a) and caudal (b) lengths from the lesion centre are also measured. L – left, R – right, Cr – cranial, Cd – caudal

Dogs without intramedullary T2W hyperintensity were classified into 'no' intramedullary T2W hyperintensity group. If one of the reviewers considered there was an absence of intramedullary T2W hyperintensity, the patient was classified into the 'no' intramedullary T2W hyperintensity group.

The length of ECM and the intramedullary T2W hyperintensity (total length, and cranial [cr] and caudal [cd] lengths from the lesion centre) were calculated as a ratio of the length of L2 (ECM length [ECML]:L2, T2W:L2, crT2W:L2, and cdT2W:L2 respectively).

On transverse T2W images at the level of lesion, the area of the ECM and area of the spinal canal were measured to calculate the occupancy ratio (OccR) by dividing the area of ECM by the area of the spinal canal. In measuring OccR, the transverse image was selected, on which the spinal cord was most compressed by EMC, from a sequential series of the images at the lesion.

On dorsal FASE image, the most extensive continuous CSF signal attenuation was identified and measured using a DICOM viewer (Figure 1). The lesion centre was located and correlated on the T1W transverse images because the signals from the vertebrae or soft tissues are not visible on FASE images (due to the nature of this sequence), and cranial (cr) and caudal (cd) extent of CSF attenuation from the centre was measured. The measured lengths (total length, and cr and cd lengths) were calculated as a ratio to the length of the L2 (CSF:L2, crCSF:L2, and cdCSF:L2, respectively).

To evaluate the relationship between the location of CSF signal attenuation and the intramedullary T2W hyperintensity, the crCSF:L2 and crT2W:L2, and the cdCSF:L2 and cdT2W:L2 were compared respectively. If differences in each comparison were less than one, then the intramedullary T2W hyperintensity and CSF attenuation were defined as a 'match' and if not, then they were classified as 'no match.'

Surgery and clinical outcome

Either mini-hemilaminectomy or hemilaminectomy was selected by the neurologists on a case by case basis. Prophylactic fenestration was performed under the decision of the surgeon. Clinical outcome in each patient was determined from the medical records or via clinical communication with the owner. Clinical outcome was classified as 'successful' or 'unsuccessful'. The outcome was considered 'successful' if the dog regained the ability to walk without assistance for more than 10 steps, voluntary urinary and faecal function and DPP in grade 3 dogs. The dogs with suspected or confirmed PM were classified as unsuccessful.

Statistical analyses

Statistical analyses were performed with commercially available software (GraphPad Prism 5, GraphPad Software Inc., La Jolla, CA, USA). *P*-values less than 0.05 were considered statistically significant. Spearman's rank correlation coefficient was used to assess correlations between CSF:L2 and T2W:L2, CSF:L2 and ECML:L2, and CSF:L2 and OccR regardless of the dog's neurological severity. The same analyses were performed in each intramedullary T2W hyperintensity subgroup to evaluate the factors influencing CSF attenuation. The Kruskal–Wallis test

was used to compare CSF:L2 and T2W:L2 among neurological grades, and the intramedullary T2W hyperintensity subgroup. The Mann–Whitney U test was used to compare CSF:L2 and T2W:L2 between the dogs with PM and those without PM among the dogs without DPP, since CSF signal attenuation and the intramedullary T2W hyperintensity in dogs with PM were previously reported to be longer than those in dogs without DPP (Castel et al. 2017, Gilmour et al. 2017). Thus, if the Mann–Whitney U test showed significance, the Kruskal–Wallis test for neurological severity among the groups was performed again after excluding the dogs with PM from grade 3.

Ethical consideration

Data was retrospectively gathered from clinical cases treated at our institution within informed consent from owners and as such ethical consideration was not required for this study.

Results

Fifty-five dogs were included in this study. Of these, 48 were Miniature Dachshunds, two were Toy Poodles, with one each of a Miniature Schnauzer, Pekingese, Shih Tzu, Bichon Frise, and mixed breed (Miniature Dachshund and Poodle). Thirty-seven dogs were male (neutered = 22 dogs), and 18 dogs were female (spayed = 12 dogs). The lesion site and case population were as follows: T11–12 (n = 3 dogs), T12–13 (n = 9), T13–L1 (n = 18), L1–2 (n = 14), L2–3 (n = 6), L3–4 (n = 4), and L4–5 (n = 1). The median age of the dogs was 9.3 years (range, 4–15), and the median body weight was 6.1 kg (range, 4.4–10). The median times between the onset of clinical signs and MRI, MRI and surgery, and the onset of clinical signs and surgery were 8 (range, 0–44), 0 (range 0–12), and 9 (range 0–44) days, respectively. Nine of 55 dogs were classified as grade 1, 33 as grade 2, and the remaining 13 dogs were grade 3. Four dogs in grade 3 were diagnosed as having concurrent PM, and two of these dogs did not undergo surgery. Decompressive surgery was performed in 53 dogs; of these, 51 dogs underwent a mini-hemilaminectomy and one dog underwent a hemilaminectomy. The remaining dog underwent an extended mini-hemilaminectomy combined with extended durotomy, which was included in another study (Jeffery et al. 2020). Therefore, this dog was excluded from assessments of the MRI findings relative to clinical outcome but was included in the evaluation of MRI findings relative to severity. All dogs in grade

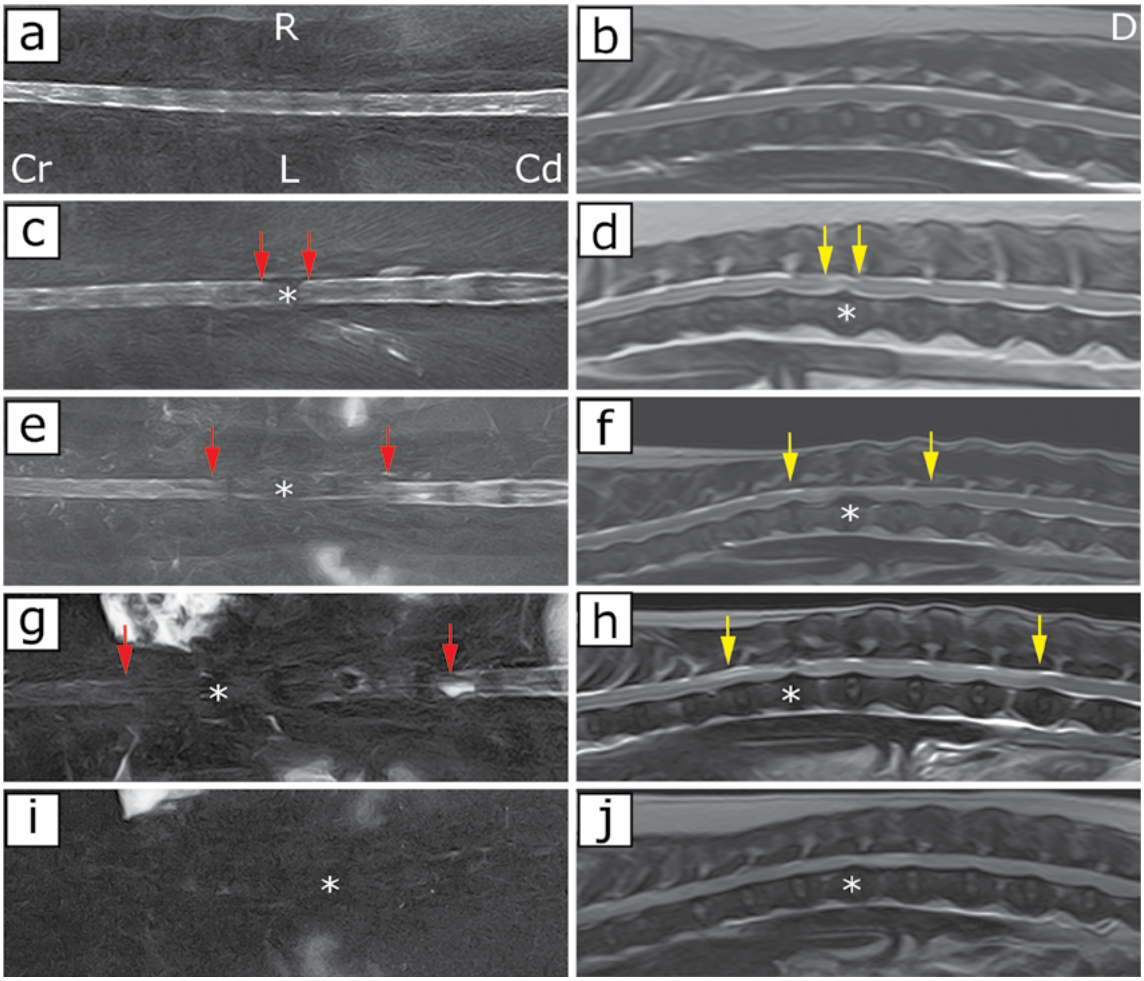

Figure 2: Combinations of images (dorsal FASE left column, sagittal T2W right column) from dogs with no spinal diseases (a,b), intervertebral disc extrusion grade 1, non-ambulatory and paraparetic dog (c,d), grade 2, paraplegic with deep pain perception (e,f), grade 3, paraplegic without deep pain perception (g,h), and PM, progressive myelomalacia (i,j). The length of cerebrospinal fluid (CSF) signal attenuation (between two red arrows) on the dorsal fast advanced spin-echo (FASE) images (a,c,e,g,i) and length of intramedullary T2W hyperintensity of the spinal cord (between two yellow arrows) (b,d,f,h,j) increases in association with increasing neurological severity. In dogs with PM, there was extensive CSF signal attenuation and intramedullary T2W hyperintensity. Cranial is the left side for the sagittal images. The dorsal FASE images (a,c,e,g,i) are purposely rotated 90 degrees to the left, to aid visual comparison to the T2W sagittal images (b,d,f,h,j). L – left, R – right, D – dorsal, Cr – cranial, Cd – caudal, asterisk – lesion site

Table I: Summary results of the numerical data for each neurological severity grade

Variable	Grade 1 (*n* = 9)		Grade 2 (*n* = 33)		Grade 3 (*n* = 13)	
	Median (mean)	Range (min ; max)	Median (mean)	Range (min ; max)	Median (mean)	Range (min ; max)
Age [years]	9.70 (9.75)	5.45 ; 12.86	9.88 (9.42)	4.16 ; 15.65	6.00 (7.37)	4.69 ; 13.4
Body weight [kg]	5.76 (6.20)	4.80 ; 8.95	5.85 (6.40)	4.35 ; 10.5	6.60 (6.49)	5.06 ; 7.70
Time from onset to MRI [days]	12.0 (15.6)	4 ; 44	9.00 (10.03)	0 ; 44	4.00 (7.15)	1 ; 31
Time from MRI to surgery [days]	0 (0.44)	0 ; 2	0 (0.70)	0 ; 10	2 (3.64)	0 ; 12
Time from onset to surgery [days]	12.0 (16.0)	4 ; 44	9.00 (10.73)	0 ; 44	7.00 (11.36)	1 ; 36
CSF:L2	1.92 (1.91)	0.64 ; 3.44	2.05 (2.27)	0.36 ; 6.41	5.75 (7.46)	2.38 ; 16.50
T2W:L2	0.66 (0.71)	0.45 ; 1.27	0.86 (1.49)	0.27 ; 6.36	4.25 (6.64)	0.83 ; 17.67
ECML:L2	0.42 (0.54)	0.26 ; 1.11	0.42 (0.51)	0.27 ; 1.24	0.42 (0.56)	0.24 ; 0.97
OccR [%]	44.0 (45.9)	16.7 ; 70.6	47.1 (44.1)	13.5 ; 74.0	60.0 (49.2)	6.84 ; 80.8

Grade 1, non-ambulatory paraparesis; grade 2, paraplegia with deep pain perception; grade 3, paraplegia without deep pain perception; min, minimum; max, maximum; CSF:L2, cerebrospinal fluid signal attenuation length as measured on the fast advanced spin-echo images and expressed as a ratio to the length of the second lumbar vertebral body (L2); T2W:L2, intramedullary T2-weighted (T2W) hyperintensity of the spinal cord length as measured on the T2W sagittal images and expressed as a ratio to the length of L2 (for this data item, 12 dogs were included in grade 3, 19 in grade 2, and five in grade 1 after excluding dogs that did not show intramedullary T2W hyperintensity); ECML:L2, extradural compressive material cranial-caudal length as measured on the T2W sagittal images and expressed as a ratio to the length of L2; OccR, occupancy ratio of the extradural compressive material in the vertebral canal as measured on the T2W transverse images. The times from onset to surgery and from MRI to surgery in grade 3 were obtained from 11 dogs because two dogs did not undergo surgery.

1, 31 of 33 dogs in grade 2, and two of 12 dogs in grade 3 (one case was excluded) were judged to have a successful outcome. Case characteristics, time between onset of clinical signs and MRI, time between onset of clinical signs and surgery, and MRI finding in each grade are summarised in Table I. CSF analysis was available in seven dogs, for which the details are summarised in Table II.

MRI findings correlating with CSF signal attenuation on FASE images

Intramedullary T2W hyperintensities of the spinal cord were detected in 36 of 55 dogs. Of these, 21 dogs were judged as having extended intramedullary T2W hyperintensity (grade 1, 1 dog; grade 2, 9 dogs; and grade 3, 11 dogs) and 15 dogs had focal intramedullary T2W hyperintensities (grade 1, 4 dogs, grade 2, 10 dogs; and grade 3, 1 dog). There was an overall significant correlation between CSF:L2 and T2W:L2 (r = 0.782, $p < 0.0001$), and CSF:L2 and ECML:L2 (r = 0.412, p = 0.0018; Table III). In the extended intramedullary T2W hyperintensity group, CSF:L2 was significantly correlated with T2W:L2 (r = 0.718, p = 0.0002) but not other MRI findings including ECML:L2 and OccR (Table III). In the focal intramedullary T2W hyperintensity group, CSF:L2 was significantly correlated with ECML:L2 (r = 0.639, p = 0.0103) but not with T2W:L2 or OccR. In the no intramedullary T2W hyperintensity group, CSF:L2 was significantly correlated with ECML:L2 (r = 0.483, p = 0.0364)

Table II: Results of cerebrospinal fluid analysis and findings of magnetic resonance imaging in seven dogs

Case	1	2	3	4	5	6	7
Grade	2	3	3	3	3	3	3
CSF:L2	6.41	2.38	4.77	4.81	16.44	5.03	16.50
T2W:L2	6.36	3.50	4.70	3.80	17.67	6.39	15.99
Match/no match	Match	No match	Match	No match	Match	No match	Match
Progressive myelomalacia	-	-	-	-	+	+	+
CSF analysis							
Colour tone	Y	Y	Y	Y	C	Y	Y
Number of nucleated cells (cell/µl)	4	1	1	4	1	2	No data
Pandy's test	P	P	P	P	N	No data	
Specific weight	1.010	1.010	1.009	1.016	1.006	No data	
pH	8	8	8	8	6	8	
Protein content (mg/dl)	Over 100	Over 30	Over 1000	Over 300	Over 300	Over 300	
Glucose (mg/dl)	Over 250	Over 250	Over 250	Over 250	Over 250	Over 100	
Haemoglobin/Occult blood	P/P	P/P	P/P	P/P	N/N	P/P	

Grade 2 – paraplegia with deep pain perception, grade 3 – paraplegia without deep pain perception, min – minimum, max – maximum, CSF:L2 – cerebrospinal fluid (CSF) signal attenuation length as measured on the fast advanced spin-echo images and expressed as a ratio to the length of the second lumbar vertebral body (L2), T2W:L2 – intramedullary T2-weighted (T2W) hyperintensity of the spinal cord length as measured on the T2W sagittal images and expressed as a ratio to the length of L2, Y – yellow transparent (xanthochromia), C – colourless transparent, P – positive, N – negative. Position of intramedullary T2W hyperintensity and position of CSF signal attenuation were considered to show a 'match' if the difference between CSF:L2 and T2WI:L2 was < 1 on the cranial and caudal side. The positions were considered 'no match' if the difference was ≥1 on at least one side. The pH, protein content, glucose level, haemoglobin level, and occult blood were measured in CSF using a urine dipstick test.

Table III: Results of statistical analysis examining the correlation between attenuation of cerebrospinal fluid signal and other magnetic resonance imaging findings

Variable	Total (n = 55)	Intramedullary T2W hyperintensity subgroup		
		Extended (21)	Focal (15)	No (19)
(CSF:L2 versus)	r (p	r (p	r (p	r (p)
T2W:L2	0.782† (< 0.0001)***	0.718 (0.0002)***	0.364 (0.1819)	-
ECML:L2	0.412 (0.0018)**	0.114 (0.6218)	0.639 (0.0103)*	0.483 (0.0364)*
OccR	0.234 (0.0856)	-0.022 (0.9243)	0.482 (0.0687)	0.111 (0.6524)

r – spearman r values, *p* – *p*-value; CSF:L2 – cerebrospinal fluid signal attenuation length as measured on the fast advanced spin-echo images and expressed as a ratio to the length of the second lumbar vertebral body (L2), T2W:L2 – intramedullary T2-weighted (T2W) hyperintensity of the spinal cord length as measured on the T2W sagittal image and expressed as a ratio to the length of L2, ECML:L2 – extradural compressive materials cranial-caudal length as measured on the T2W sagittal images and expressed as a ratio to the length of L2, OccR – occupancy ratio of the extradural compressive materials in the vertebral canal as measured on the T2W transverse images. Extended intramedullary T2W hyperintensity group, T2W:L2 ≥1; focal intramedullary T2W hyperintensity group, T2W:L2 1 > and > 0; no intramedullary T2W hyperintensity group, absent intramedullary T2W hyperintensity.
†, The number of cases with intramedullary T2W hyperintensity was 36.
*, $p < 0.05$; **, $p < 0.01$; ***, $p < 0.001$

Table IV: Clinical outcome and measurement values for magnetic resonance imaging findings in paraplegic dogs with or without deep pain perception

	Clinical outcome					
	Successful			Unsuccessful		
Variable	*n*	Median (mean)	Range (min ; max)	*n*	Median (mean)	Range (min ; max)
CSF:L2						
Grade 2 (*n* = 33)	31	2.05 (2.16)	0.36 ; 6.41	2	3.93 (3.93)	1.54 ; 6.31
Grade 3 (*n* = 12)	2	3.72 (3.72)	3.65 ; 3.80	10	5.91 (8.34)	2.38 ; 16.50
T2W:L2						
Grade 2 (*n* = 19)	17	1.00 (1.60)	0.43 ; 6.36	2	0.54 (0.54)	0.27 ; 0.81
Grade 3 (*n* = 11)	2	1.40 (1.40)	0.83 ; 1.96	9	4.70 (7.91)	1.41 ; 17.67

n – number of dogs, min – minimum, max – maximum, grade 2 – paraplegia with deep pain perception (DPP), grade 3 – paraplegia without DPP, CSF:L2 – cerebrospinal fluid signal attenuation length as measured on the fast advanced spin-echo images and expressed as a ratio to the length of the second lumbar vertebral body (L2), T2W:L2 – intramedullary T2-weighted (T2W) hyperintensity of the spinal cord length as measured on the T2W sagittal images and expressed as a ratio to the length of L2. Outcome was considered successful if the dog showed the ability to walk without assistance for more than 10 steps, the presence of DPP, and voluntary fecal and urinary function.

but not with OccR. The CSF:L2 varied significantly among the different groups of the intramedullary T2W hyperintensity ($p < 0.0001$). The CSF:L2 in dogs with the extended intramedullary T2W hyperintensities was significantly larger than those in the focal or no intramedullary T2W hyperintensity groups ($p < 0.001$ and $p < 0.05$, respectively).

Of 21 dogs classified as the extended intramedullary T2W hyperintensity group, 12 dogs were considered to be a match (grade 1, 1/1 dog; grade 2, 6/9 dogs; and grade 3, 5/11 dogs); of the 15 dogs in the focal intramedullary T2W hyperintensity group, 10 dogs were considered to be a match (grade 1, 3/4 dogs; grade 2, 7/10 dogs; and grade 3, 0/1 dog).

Neurological severity, MRI findings, and clinical outcome

Significant differences were detected in CSF:L2 according to neurological grade ($p < 0.0001$; Figure 2 and Table I). The CSF:L2 in grade 3 was significantly larger than those in grades 1 or 2 (both; $p < 0.001$) but there was no significant difference between grade 1 and grade 2. Similarly, the T2W:L2 in grade 3 was larger than those of grade 1 or 2 (among the groups $p = 0.0003$, grade 3 vs 1 and grade 3 vs 2; $p < 0.01$ each).

In comparing dogs with and without PM in the grade 3 sub category, the CSF:L2 and T2W:L2 were larger in dogs with concurrent PM than those without PM ($p = 0.0336$; median 15.72 vs 4.81, and $p = 0.004$; median 15.18 vs 3.43).

Excluding dogs with PM from the population of grade 3, there were significant differences in CSF:L2 and T2W:L2 among neurological grades ($p = 0.0003$, $p = 0.0054$ respectively). The CSF:L2 and T2W:L2 in dogs classified as grade 3 were larger than those classified as grade 1 or 2 (CSF:L2: grade 1 vs 3, $p < 0.01$, grade 2 vs 3, $p < 0.001$; and T2W:L2: grade 1 vs 3, $p < 0.01$, grade 2 vs 3, $p < 0.05$).

In this study, the case population was too small to perform statistical analyses evaluating for the association between MRI findings and clinical outcomes (Table IV). However, subjectively, the dogs determined to be in the unsuccessful group tended to have larger CSF:L2 than those with a successful outcome (grade 2: median 3.93 vs 2.05, grade 3: median 5.91 vs 3.72). When evaluating patients in the grade 3 group, the unsuccessful subgroup tended to have a larger T2W:L2 than those in the successful subgroup (median 4.70 vs 1.40). When evaluating patients in the grade 2 group, the successful subgroup surprisingly tended to have a larger T2W:L2 than those in the unsuccessful subgroup (median 1.00 vs 0.54).

Discussion

In this retrospective study, we demonstrate that, compared to dogs with DPP, paraplegic dogs without DPP have extended CSF signal attenuation on FASE sequence, which are significantly correlated with extended intramedullary T2W hyperintensity of the spinal cord, which may indicate spinal cord swelling. In dogs with DPP, CSF signal attenuation was more focal and thought to

be due to extradural compression of the spinal subarachnoid space by ECM because of the significant correlation between CSF:L2 and ECML:L2. The OccR was not significantly correlated with neurological grade, CSF attenuation, intramedullary T2W hyperintensity, or outcome (see supplemental file for relation of the OccR and outcome). These findings indicate that the severity of spinal cord compression might not be related to the neurological severity and/or outcome, as similar to a previous study (Besalti et al. 2006), in addition to spinal cord swelling.

It has been reported that spinal cord injury could be classified into two phases; i) primary injury, which results from mechanical trauma to the neural tissues resulting in axon damage, demyelination, and haemorrhage (Griffiths 1978; Janssens 1991; Smith & Jeffery 2006), and followed by ii) secondary injury such as cytotoxic oedema and oncotic swelling due to neural tissue destruction, free radical formation, and inflammation (Janssens 1991; Olby 2010). The pathophysiological events in secondary injury result in intramedullary T2W hyperintensity of the spinal cord on MRI (Jeffery et al. 2013; Narayana et al. 1999, 2004; Purdy et al. 2003, 2004).

In dogs with TL-IVDE, neurological dysfunction could occur due to primary and secondary injuries after spinal cord compression by the extruded nucleus pulposus (Griffiths 1978; Janssens 1991; Jeffery et al. 2013). It is currently widely accepted that prognosis in paraplegic dogs without DPP is poor due to severe damage to the spinal cord (Henke et al. 2013; Ito et al. 2005; Jeffery et al. 2013, 2016; Smith & Jeffery 2006), and severely damaged spinal cord would regularly show gross swelling (Jeffery et al. 2020; Takahashi et al. 2020). In these cases, spinal cord injury (swelling) would be a main cause of neurological dysfunction, which is supported by previous imaging studies investigating diffuse intramedullary T2W hyperintensity (Alisauskaite et al. 2017; Boekhoff et al. 2012; Ito et al. 2005; Levine et al. 2009) and studies demonstrating the lack of association between the degree of spinal cord compression and severity/outcome (Besalti et al. 2006; Penning et al. 2006). Furthermore, it has been reported that spinal cord swelling could be evaluated on myelography in dogs without DPP due to extradural compressive myelopathy secondary to TL-IVDE by visualising attenuation of contrast medium in the spinal subarachnoid space (Duval et al. 1996). Therefore, based on the significant correlation between CSF:L2 and T2W:L2 shown in this study, it can be concluded that extended CSF signal attenuation on FASE images, especially in grade 3 patients, is more likely to be as a result of spinal cord swelling.

Although it was not possible to perform statistical processing, grade 3 dogs that had a poor outcome tended to have greater CSF:L2 and T2W:L2 (median 5.91 and 4.70, respectively), which is similar to previous studies (Duval et al. 1996; Ito et al. 2005). Previous myelographic studies in paraplegic dogs without DPP due to TL-IVDE, showed that if the length of the most attenuated contrast column was more than five times the length of L2, then there was a poor prognosis (Duval et al. 1996); alternatively, on MRI, a ratio of the length of the intramedullary T2W hyperintensity mid-sagittal images to the length of L2 of more than 3 was indicative of a poor prognosis (Ito et al. 2005). Based on those studies, our results indicate that extended spinal cord swelling would be related to a poor outcome, and they support the use of extended durotomy as a reasonable treatment, which has been reportedly performed recently in dogs with TL-IVDE without DPP (Jeffery et al. 2020). Grade 2 dogs had greater T2W:L2, which was in contrast with those of grade 3. It has been reported that in paraplegic dogs with DPP caused by intervertebral diseases, longer intramedullary T2W hyperintensity indicated poor prognosis (Ito et al. 2005). However, the other report has described no significant relation between the T2 hyperintensity and motor function recovery (Wang-Leandro et al. 2017). Therefore, it could be possible that, in grade 2 dogs, the intramedullary T2W hyperintensity reflects reversible pathological changes of the spinal damage.

It has been reported that extradural spinal cord compression due to extruded disc also causes CSF attenuation on heavily T2W images (Guillem Gallach et al. 2011; Mankin et al. 2012; Pease et al. 2006). In our study, in cases with focal CSF signal attenuation on FASE images, the attenuation of CSF signal was thought to be due to compression of the subarachnoid space by ECM because of the significant correlation observed between the CSF:L2 and ECML:L2.

In 22/36 cases (61%), the location of CSF signal attenuation on the FASE image and the intramedullary T2W hyperintensity was judged as a 'match'. Five of 14 dogs classified as 'no match' showed focal intramedullary T2W hyperintensity of the spinal cord. Median CSF:L2 (2.36) in these five dogs was larger than T2W:L2 (0.58), ECML:L2 (0.66) and OccR (0.66). In these cases, CSF:L2 was not correlated with ECML:L2 and OccR (both, p = 0.35). The remaining nine dogs classified as 'no match' showed extended intramedullary T2W hyperintensity. Of these, six dogs had larger CSF:L2 (median, 5.28) than T2W:L2 (2.59), and the remaining three dogs had larger T2W:L2 (3.50) than CSF:L2 (2.38). Although the precise reasons for this mismatch are not apparent, the severity of spinal cord swelling, and/or cell population and protein concentration in the CSF could be the underlying causes.

The cause of the mismatch in dogs with larger CSF:L2 attenuation in both sub-groups (focal, five dogs; extended, six) is uncertain and unexplainable. Previously, it has been reported that elevated concentrations of protein (143 mg/dL) and increased cell populations (white blood cells: 553/μL; red blood cells: 440/μL) in the CSF had affected the heavily T2W images, attenuating CSF signal on the images, in dogs with meningomyelitis (Pease et al. 2006).

Therefore, it could be possible that in our cases, with larger CSF:L2 attenuation in the 'no match' group, the changes in CSF composition could affect the CSF signal on FASE images. However, there were also contradictions in our cases that some dogs with elevated concentrations of protein and increased cell populations had larger T2W:L2 (Table II; case 2 and 6).

While in three dogs with a larger T2W:L2 in the 'no match' group, the subarachnoid space at the cranial and caudal edge of the intramedullary T2W hyperintensity was apparent on T2W images (data not shown). Therefore, in these cases, spinal cord swelling might not be enough to compress the subarachnoid space in the lesion where intramedullary T2W hyperintensity of the spinal

cord was detected. In these areas, the CSF signal was detectable on FASE images but the intramedullary T2W hyperintensity was also detectable at the same level (resulting in a longer length of the intramedullary T2W hyperintensity than the CSF signal attenuations).

The length of CSF signal attenuation on FASE images in dogs with concurrent PM was significantly longer than those in dogs without PM (median CSF:L2, 15.72 vs 4.81 respectively, $p = 0.034$), similar to previous studies (Castel et al. 2017; Gilmour et al. 2017). However, in comparison with previous PM cases without DPP (median CSF:L2, 8.9 [Gilmour et al. 2017]), dogs with PM in this present study had a longer length of CSF attenuation on heavily T2W images. It has been reported that the length of intramedullary T2W hyperintensity of the spinal cord would increase with time after the onset of neurological signs in dogs with presumptive PM (Takahashi et al. 2020). The progression of this imaging finding would reflect the pathophysiological stage of PM that consists of progressive ascending and/or descending haemorrhagic necrosis of the spinal cord after severe spinal cord contusive injury (Griffiths 1972). In a previous study (Gilmour et al. 2017), images were obtained a relatively short period after the onset of neurological signs (median 2 days; range 1–14 days), but in our cases the images were acquired at a more distant time point after onset (median 4 days; range 4–8 days). This might cause larger CSF signal attenuation in dogs with PM in the present study than that in the previous study.

The present study was not without limitations. Histopathological examinations of the spinal cords were not performed. Therefore, we could not determine how accurately the MRI findings of intramedullary T2W hyperintensity reflected pathological changes in the spinal cord (i.e. spinal cord swelling). In addition, as the data relating on intraoperative gross findings of the spinal cord and extradural compressive lesions, including extruded disc material and haemorrhage were not obtained from medical records, we could not conclude if the spinal cords were grossly swollen at the lesion sites, and if ECM consisted only of extruded disc materials (and not others, such as haematoma). Additionally, CSF examination was not performed in most dogs. Thus, we could not investigate how changes in CSF composition could have affected the attenuation of CSF signals on FASE images.

Further research to investigate the relationship between CSF signal attenuation on heavily T2W images and the prognosis of dogs with IVDE using a larger number of cases is necessary. However, because the dogs without DPP that show an extended CSF signal attenuation would have a poor prognosis, the treatment options and potential outcomes would need to be thoroughly explained to the owner. In addition, when the locations of the CSF signal attenuation and intramedullary T2W hyperintensity of the spinal cord did not match, concurrent pathological changes of the spinal cord, which can change the composition of CSF, such as inflammation and haemorrhage (i.e. spinal cord injury) following disc herniation (Levine et al. 2014, Wistberger et al. 2012), could be suspected. In these cases, CSF analysis might be recommended because elevated cell population and protein concentration in CSF would affect the outcome (Levine et al. 2014, Wistberger et al. 2012).

Conclusion

In dogs with IVDE, the length of CSF signal attenuation on FASE image was correlated with and caused by compression by ECM or intramedullary hyperintensity of the spinal cord on T2W images. Extended attenuation of CSF signal more likely to be caused by spinal cord swelling, noted on MRI images as intramedullary T2W hyperintensity. The extended attenuation is associated with presurgical neurological severity and was associated with poorer clinical outcomes after decompression surgery.

Acknowledgements

The authors would like to acknowledge the work of members of their laboratory and veterinary residents at their institution.

Conflict of interest

The authors have declared that no competing interests exist.

Funding source

The authors received no financial support for the research, authorship, and/or publication of this article.

Ethical approval

Data was retrospectively gathered from clinical cases treated at our institution within informed consent from owners and as such ethical consideration was not required for this study.

ORCID

N Sekiguchi https://orcid.org/0000-0001-8307-8898
D Ito https://orcid.org/0000-0002-3671-1889
C Ishikawa https://orcid.org/0000-0002-2555-0071
N Tanaka https://orcid.org/0000-0002-6928-9768
M Kitagawa https://orcid.org/0000-0001-9052-5254

Appendix

Equivalent sequences of FASE in other MRI brands

Half-Founder Acquisition Single-shot Turbo spin Echo (**HASTE**) imaging (**Siemens**), Single-shot fast spin echo (SS-FSE) (**GE**), Single-shot turbo spin echo (SSH-TSE) or ultra-fast spin echo (UFSE) (**Philips**), and Single-shot fast SE (**Hitachi**).

References

Aggarwal, A., Azad, R., Ahmad, A., et al., 2012, Additional merits of two-dimensional single thick-slice magnetic resonance myelography in spinal imaging, *Journal of Clinical Imaging Science* 84(2), 1–5. https://doi.org/10.4103/2156-7514.105268.

Alisauskaite, N., Spitzbarth, I., Baumgärtner, W., et al, 2017, Chronic post-traumatic intramedullary lesions in dogs, a translational model', *PLoS One* 12(11), e0187746. https://doi.org/10.1371/journal.pone.0187746.

Besalti, O., Pekcan, Z., Sirin, Y.S., et al., 2006, Magnetic resonance imaging findings in dogs with thoracolumbar intervertebral disk disease: 69 cases (1997–2005)' *Journal of the American Veterinary Medical Association* 228(6), 902–908. https://doi.org/10.2460/javma.228.6.902.

Boekhoff, T.M., Flieshardt, C., Ensinger, E., et al., 2012, Quantitative magnetic resonance imaging characteristics: evaluation of prognostic value in the dog as a translational model for spinal cord injury, *Journal of Spinal Disorders & Techniques* 25(3), E81–E87. https://doi.org/10.1097/BSD.0b013e31823f2f55.

Castel, A., Olby, N.J., Mariani, C.L., et al., 2017, Clinical characteristics of dogs with progressive myelomalacia following acute intervertebral disk extrusion, *Journal of Veterinary Internal Medicine* 31(6), 1782–1789. https://doi.org/10.1111/jvim.14829.

De Risio, L., Adams, V., Dennis, R., et al., 2009, Association of clinical and magnetic resonance imaging findings with outcome in dogs with presumptive acute noncompressive nucleus pulposus extrusion: 42 cases (2000–2007), *Journal of the American Veterinary Medical Association* 234(4), 495–504. https://doi.org/10.2460/javma.234.4.495.

Duncan, S.M., Amrhein T.J., 2012, T2 Contrast, in W.I. Mangrun & K.L. Christianson (eds.), *Duke review of MRI principles*, pp. 19–41, Elsevier Mosby, Philadelphia. https://doi.org/10.1016/B978-1-4557-0084-4.00002-4.

Duval, J., Dewey, C., Roberts, R., et al., 1996, Spinal cord swelling as a myelographic indicator of prognosis: a retrospective study in dogs with intervertebral disk disease and loss of deep pain perception, *Veterinary Surgery* 25(1), 6–12. https://doi.org/10.1111/j.1532-950X.1996.tb01371.x.

Gilmour, L.J., Jeffery, N.D., Miles, K., et al., 2017, Single-shot turbo spin echo pulse sequence findings in dogs with and without progressive myelomalacia, *Veterinary Radiology & Ultrasound* 58(2), 197–205. https://doi.org/10.1111/vru.12463.

Griffiths, I.R., 1972, The extensive myelopathy of intervertebral disc protrusions in dogs ('the ascending syndrome'), *Journal of Small Animal Practice* 13(8), 425–437. https://doi.org/10.1111/j.1748-5827.1972.tb06870.x.

Griffiths, I.R., 1978, Spinal cord injury: a pathological study of naturally occurring lesions in the dog and cat, *Journal of Comparative Pathology* 88(2), 303–315. https://doi.org/10.1016/0021-9975(78)90033-6.

Guillem Gallach, R., Suran, J., Cáceres, A.V., et al., 2011, Reliability of T2-weighted sagittal magnetic resonance images for determining the location of compressive disk herniation in dogs, *Veterinary Radiology & Ultrasound* 52(5), 479–486. https://doi.org/10.1111/j.1740-8261.2011.01833.x.

Henke, D., Vandevelde, M., Doherr, M.G., et al., 2013, Correlations between severity of clinical signs and histopathological changes in 60 dogs with spinal cord injury associated with acute thoracolumbar intervertebral disc disease, *The Veterinary Journal* 198(1), 70–75. https://doi.org/10.1016/j.tvjl.2013.04.003.

Ito, D., Matsunaga, S., Jeffery, N.D., et al., 2005, Prognostic value of magnetic resonance imaging in dogs with paraplegia caused by thoracolumbar intervertebral disk extrusion: 77 cases (2000–2003), *Journal of the American Veterinary Medical Association* 227(9), 1454–1460. https://doi.org/10.2460/javma.2005.227.1454.

Ito, D., Ishikawa, C., Sekiguchi, N., et al., 2020, Utility of "MR myelograohy" in diagnosis of a presumed spinal subarachnoid diverticulum, *Journal of Small Animal Practice* 61(12), 782. https://doi.org/10.1111/jsap.13208.

Janssens, L.A.A., 1991, Mechanical and pathophysiological aspects of acute spinal cord trauma, *Journal of Small Animal Practice* 32(11), 572–578. https://doi.org/10.1111/j.1748-5827.1991.tb00889.x.

Jeffery, N.D., Levine, J.M., Olby, N.J., et al., 2013, Intervertebral disk degeneration in dogs: consequences, diagnosis, treatment, and future directions, *Journal of Veterinary Internal Medicine* 27(6), 1318–1333. https://doi.org/10.1111/jvim.12183.

Jeffery, N.D., Barker, A.K., Hu, H.Z., et al., 2016, Factors associated with recovery from paraplegia in dogs with loss of pain perception in the pelvic limbs following intervertebral disk herniation, *Journal of the American Veterinary Medical Association* 248(4), 386–394. https://doi.org/10.2460/javma.248.4.386.

Jeffery, N.D., Mankin, J.M., Ito, D., et al., 2020, Extended durotomy to treat severe spinal cord injury after acute thoracolumbar disk herniation in dogs, *Veterinary Surgery* 49(5), 884–893. https://doi.org/10.1111/vsu.13423.

Levine, G.J., Cook, J.R., Kerwin, S.C., et al., 2014, Relationships between cerebrospinal fluid characteristics, injury severity, and functional outcome in dogs with and without intervertebral disk herniation, *Veterinary Clinical Pathology* 43(3), 437–446. https://doi.org/10.1111/vcp.12165.

Levine, J.M., Fosgate, G.T., Chen, A.V., et al., 2009, Magnetic resonance imaging in dogs with neurologic impairment due to acute thoracic and lumbar intervertebral disk herniation, *Journal of Veterinary Internal Medicine* 23(6), 1220-1226. https://doi.org/10.1111/j.1939-1676.2009.0393.x.

Mankin, J.M., Hecht, S., Thomas, W.B., 2012, Agreement between T2 and haste sequences in the evaluation of thoracolumbar intervertebral disk disease in dogs, *Veterinary Radiology & Ultrasound* 53(2), 162–166. https://doi.org/10.1111/j.1740-8261.2011.01894.x.

Nagayama, M., Watanabe, Y., Okumura, A., et al., 2002, High-resolution single-slice MR myelography, *American Journal of Roentgenology* 179(2), 515–521. https://doi.org/10.2214/ajr.179.2.1790515.

Narayana, P., Abbe, R., Liu, S.J., et al., 1999, Does loss of gray- and white-matter contrast in injured spinal cord signify secondary injury? In vivo longitudinal MRI studies, *Magnetic Resonance in Medicine* 41(2), 315–320. https://doi.org/10.1002/(SICI)1522-2594(199902)41:2<315::AID-MRM15>3.0.CO;2-B.

Narayana, P.A., Grill, R.J., Chacko, T., et al., 2004, Endogenous recovery of injured spinal cord: longitudinal in vivo magnetic resonance imaging, *Journal of Neuroscience Research* 78(5), 749–759. https://doi.org/10.1002/jnr.20275.

Olby, N., 2010, The pathogenesis & treatment of acute spinal cord injuries in dogs' *Veterinary Clinics of North America: Small Animal Practice* 40(5), 791–807. https://doi.org/10.1016/j.cvsm.2010.05.007.

Okada, M., Kitagawa, M., Ito, D., et al., 2010, Magnetic resonance imaging features and clinical signs associated with presumptive and confirmed progressive myelomalacia in dogs: 12 cases (1997–2008), *Journal of the American Veterinary Medical Association* 237(10), 1160–1165. https://doi.org/10.2460/javma.237.10.1160.

Pease, A., Sullivan, S., Olby, N., et al., 2006, Value of a single-shot turbo spin-echo pulse sequence for assessing the architecture of the subarachnoid space and the constitutive nature of cerebrospinal fluid, *Veterinary Radiology & Ultrasound* 47(3), 254–259. https://doi.org/10.1111/j.1740-8261.2006.00136.x.

Penning, V., Platt, S.R., Dennis, R., et al., 2006, Association of spinal cord compression seen on magnetic resonance imaging with clinical outcome in 67 dogs with thoracolumbar intervertebral disc extrusion, *Journal of Small Animal Practice* 47(11), 644–650. https://doi.org/10.1111/j.1748-5827.2006.00252.x.

Purdy, P.D., Duong, R.T., White, C.L. 3rd, et al., 2003, Percutaneous translumbar spinal cord compression injury in a dog model that uses angioplasty balloons: MR imaging and histopathologic findings, *American Journal of Neuroradiology* 24(2), 177–184.

Purdy, P.D., White, C.L. 3rd, Baer, D.L., et al., 2004, Percutaneous translumbar spinal cord compression injury in dogs from an angioplasty balloon: MR and histopathologic changes with balloon sizes and compression times, *American Journal of Neuroradiology* 25(8), 1435–1442.

Seiler, G.S., Robertson, I.D., Mai, W., et al, D.E., 2012, Usefulness of a half-fourier acquisition single-shot turbo spin-echo pulse sequence in identifying arachnoid diverticula in dogs, *Veterinary Radiology & Ultrasound* 53(2), 157–161. https://doi.org/10.1111/j.1740-8261.2011.01893.x.

Smith, P.M., Jeffery, N.D., 2006, Histological and ultrastructural analysis of white matter damage after naturally-occurring spinal cord injury, *Brain Pathology* 16(2), 99–109. https://doi.org/10.1111/j.1750-3639.2006.00001.x.

Takahashi, F., Honnami, A., Toki, M., et al., 2020, Effect of durotomy in dogs with thoracolumbar disk herniation and without deep pain perception in the hind limbs, *Veterinary Surgery* 49(5), 860–869. https://doi.org/10.1111/vsu.13409.

Wang-Leandro, A., Siedenburg, J.S., Hobert, M.K., et al., 2017, Comparison of preoperative quantitative magnetic resonance imaging and clinical assessment of deep pain perception as prognostic tools for early recovery of motor function in paraplegic dogs with intervertebral disk herniations, *Journal of Veterinary Internal Medicine* 31(3), 842–848. https://doi.org/10.1111/jvim.14715.

Wistberger, T.H., Levine, J.M., Fosgate, G.T., et al., 2012, Associations between cerebrospinal fluid biomarkers and long-term neurologic outcome in dogs with acute intervertebral disk herniation, *Journal of the American Veterinary Medical Association* 240(5), 555–562. https://doi.org/10.2460/javma.240.5.555.

Supplemental table: Clinical outcome, occupancy ratio, and length of extruded compressive materials

	Clinical outcome			
	Successful (*n* = 42)		**Unsuccessful (*n* = 12)**	
	Median (mean)	**Range**	**Median (mean)**	**Range**
OccR	0.46 (0.45)	0.13–0.77	0.44 (0.46)	0.07–0.81
ECML:L2	0.42 (0.52)	0.27–1.24	0.40 (0.51)	0.24–0.97

OccR – occupancy ratio of the extradural compressive material in the vertebral canal as measured on the T2W transverse images, ECML:L2 – extradural compressive material cranial-caudal length as measured on the T2W sagittal images and expressed as a ratio to length of the second lumbar vertebra. Outcome was considered successful if the dog showed the ability to walk without assistance for more than 10 steps, the presence of DPP, and voluntary fecal and urinary function.